THE AMERICAN MINERALOGIST, VOL. 52, MAY–JUNE, 1967

CHARACTERISTICS OF SYNTHETIC EMERALDS

E. M. Flanigen, D. W. Breck,[1] N. R. Mumbach and A. M. Taylor[2]

Tonawanda Research Laboratory, Union Carbide Corporation, Linde Division, Tonawanda, New York.

Abstract

Large single crystals of synthetic emerald have been grown by both hydrothermal and molten flux techniques. The synthetic hydrothermal emeralds are of excellent quality comparable to the finest natural gemstones from Colombia and the Ural Mountains. Emeralds grown from Li-molybdate, V_2O_5 and Li-tungstate fluxes are described. Their reported properties are: density, optical properties, inclusions, fluorescence behavior, chemical composition and structure, and infrared spectra. The characteristics of the new synthetic emeralds and those produced by Chatham, Gilson, Zerfass and Lechleitner are described and reviewed, and distinctions outlined. The origin of an emerald, natural, synthetic flux, or synthetic hydrothermal, can be defined by determination of characteristic properties.

Introduction

Renewed interest in synthetic emerald during the last several years has been evidenced by an increase in the number of discussions in the technical literature and by the appearance of several new synthetic emeralds on the market. The upsurge of activity in the area of synthetic emerald appears to be due both to its utility as a gemstone and its reported use as a solid state maser crystal (Goodwin, 1961). Research reported here has been concerned with the growth of synthetic emeralds by both molten flux and hydrothermal techniques. This paper describes the characteristics of the synthetic emeralds grown in this Laboratory as well as a comprehensive review and characterization of the synthetic emeralds now available commercially.

Historical Review

Since the times of Geber many scientific investigations have been conducted for aesthetic and pecuniary reasons. Like the diamond, emerald has been the object of many attempted syntheses. The earliest report of the synthesis of emerald is that of Ebelman (1848) who obtained small hexagonal prisms by heating powdered natural emerald in fused boric acid. More successful experiments by Hautefeuille and Perrey (1888, 1890) resulted in the growth of emerald prisms 1 mm in length from molten lithium molybdate or lithium vanadate containing the dissolved oxides at 800°C. Traube (1894) reported the crystallization of colorless beryl prisms by heating a gel, of the composition $Be_3Al_2Si_6O_{18} \cdot XH_2O$,

[1] Present address: Union Carbide Research Institute, Tarrytown, New York.

[2] Present address: Division of Applied Mineralogy, C.S.I.R.O., Melbourne, Australia.

which he prepared from $BeSO_4$, $Al_2(SO_4)_3$, and sodium metasilicate, with anhydrous boric acid (boron trioxide).

The I. G. Farben-Industrie conducted experimental work on the synthesis of emerald at Bitterfeld during the period 1911 to 1942. Small scale production of synthetic emerald crystals was achieved. These were marketed under the trade name "Igmerald." The properties of Igmerald have been described by Schiebold (1935), Espig and Jaeger (1935), and Anderson (1935). Details of the process were reported by Espig (1960). It is based upon the isothermal diffusion of the oxides in a lithium molybdate melt and growth on seed crystals floated beneath the surface.

Synthetic emeralds have been manufactured in the United States for about 20 years by C. F. Chatham using a process which has not been revealed. However, physical properties suggest that the crystals are self-nucleated and grown from a molten flux.

At the Mineralogical Institute in Frankfurt, Nacken grew emerald crystals by a hydrothermal process using weakly alkaline solutions containing BeO,Al_2O_3, and SiO_2 in 30 cm^3 autoclaves at 370–400°C (van Praagh, 1947; Webster, 1962). More recently Linares *et al* (1962) and Lefever *et al* (1962) have shown that beryl crystals can be grown from a variety of molten fluxes. A fusion process was suggested by the results of Amstutz and Borloz (1935) who reported the crystallization of emerald by dropping a powder mixture of BeF_2, BeO, Al_2O_3, and SiO_2 onto a seed crystal contained in an electric furnace. Gentile *et al* (1963) recently claimed the flame fusion synthesis of emerald. A photograph shows a boule section coated with mullite yet the authors claim, without presenting any evidence, that emerald melts congruently. Miller and Mercer (1965) in a recent study of the melting relationships of beryl confirm that it melts incongruently, and that all attempts to crystallize beryl from a melt or glass were unsuccesful. Growth of single crystal beryl and emerald from its melt at high temperature and pressure has been reported by Wilson (1965). Emel'yanova *et al* (1965) describe the hydrothermal growth of single crystal beryl containing V, Mn, Co and Ni, on a natural beryl seed plate at 600°C, 1500 atmospheres, from solutions of H_3BO_3 and $Na_2B_4O_7$.

Two more synthetic emeralds have recently become available commercially. One, referred to as the Gilson emerald, is manufactured by Pierre Gilson, Pas de Calais, France and is unquestionably grown from a molten flux. Another, synthesized by W. Zerfass of Idar Oberstein, is believed by Gubelin (1964) to be grown hydrothermally. However, we believe it is also grown from a molten flux. Properties of these emeralds have been described by Liddicoat (1964), Schlossmacher (1963), Gubelin (1964), and Webster (1964). A process for coating preformed cut stones of

beryl, which is believed to be hydrothermal, was developed by J. Lechleitner in Austria. These stones have been referred to as "Emerita" and for a short period were marketed in the U. S. by Union Carbide Corporation, Linde Division, as a natural beryl stone overgrown with synthetic emerald (Holmes and Crowningshield, 1960).

Research on the synthesis of emerald initiated at Linde several years ago has culminated in a process for hydrothermal growth of large, single crystals of high-quality emerald.[1]

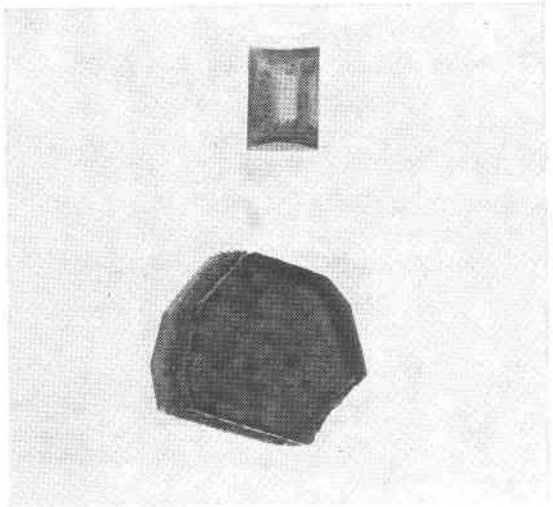

FIG. 1. Synthetic emeralds grown from Li-molybdate flux. As-grown tabular hexagonal prism crystal, 8.5 ct., 0.5% Cr. Faceted stone, lens-cut crown, step-cut pavilion, 1.13 ct., 0.09% Cr.

NEW SYNTHETIC EMERALDS

The new synthetic emeralds described here were grown by fluxmelt and hydrothermal crystal growth methods. In the case of the fluxmelt, crystals have been grown from V_2O_5, lithium molybdate and lithium tungstate fluxes, by both thermal gradient and slow cooling techniques. Growth temperatures were in the region of 900° to 1200°C in V_2O_5 and lithium tungstate, and 700°C to 900°C in lithium molybdate. Crystals as large as 25 carats have been grown. A rough synthetic emerald 8.5 carats in size grown from lithium molybdate is shown in Figure 1 together with a 1.13 carat lens shaped gemstone faceted from a similar rough crystal (0.09% Cr). To avoid excessive flux inclusions and to utilize the fast

[1] Flanigen, E. M. and Mumbach, N. R., to be published.

growth rate in the *c*-axis direction, a seed plate cut ⊥ to the *c*-axis was normally used resulting in a hexagonal prism shaped crystal. Chromium concentration varied from 0.05 to 1.4% Cr.

The hydrothermal emeralds are initially grown on a natural aquamarine or beryl seed plate. The new growth is cut from the seed plate and used subsequently as a seed plate for the synthetic emerald. The growth process results in tabular shaped crystals bounded by dipyramid and prism faces. Crystals as large as 17 carats have been grown. Faceted

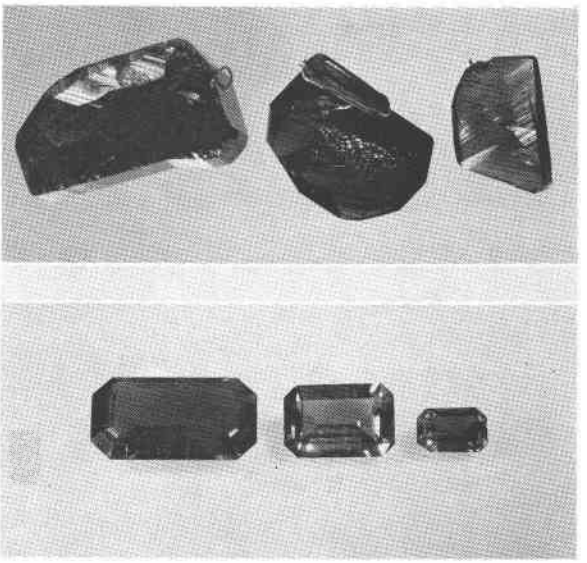

FIG. 2. Synthetic hydrothermal emeralds. As-grown crystals, 2.52, 6.77 and 11.42 carats. Faceted stones, step-cut, 0.38, 1.5 and 3.3 ct.

emeralds cut from the hydrothermal rough stones show unusually high optical quality and excellent color, leading to a high degree of brilliance. The chromium level is easily varied in the process and emeralds containing from 0.2–1.2% Cr have been grown. For gem purposes 0.2–0.4% Cr seems to result in the most aesthetically pleasing color. Several as-grown crystals and faceted stones are shown in Figure 2.

PROPERTIES

Detailed characterization of the hydrothermal emeralds and fluxmelt emeralds grown from lithium molybdate, lithium tungstate and vanadium pentoxide in this Laboratory was carried out. In addition, several other emeralds were examined. These include: a natural Colombian emerald prism, as-grown Chatham emerald prisms, two Gilson emeralds,

and several Lechleitner emerald products, "Emerita" composed of a natural beryl seed with a thin overlay of synthetic emerald, the recent beryl-emerald wafer composite, and a fully snythetic emerald obtained as an experimental sample from Lechleitner in 1962. Characterization of the emeralds from this Laboratory includes optical and density properties, X-ray diffraction and infrared spectra, fluorescence characteristics, and chemical composition.

TABLE 1. SUMMARY OF OPTICAL AND DENSITY DATA FOR SYNTHETIC EMERALD

Producer and method	Refractive index		Birefringence	Specific gravity
	ω	ϵ		
Linde, hydrothermal emerald (0.3–1.2% Cr)	1.571–1.578	1.566–1.572	0.005–0.006	2.67–2.69
Linde, hydrothermal beryl, colorless	1.569	1.563	0.006	2.66
Lechleitner, hydrothermal				
(a) emerald-coated natural beryl (1962) (pale green)	1.582–1.586	1.577–1.580	0.005–0.006	n.d.
(b) emerald-coated natural beryl (1964) (deeper green)	1.586–1.597	1.580–1.587	0.006–0.010	n.d.
(c) fully synthetic emerald (1962)	1.577	1.571–1.572	0.005–0.006	2.67–2.69
(d) fully synthetic beryl-emerald composite (1964)	1.567–1.573	1.562–1.567	0.005–0.006	2.67–2.69
Linde, flux, Li-molybdate (0.2–0.5% Cr)	1.564	1.561	0.003	2.64–2.65
V_2O_5 (0.5–1.5% Cr)	1.564–1.572	1.561–1.562	0.003–0.005	2.65–2.66
V_2O_5 no Cr	1.563	1.560	0.003	2.64–2.65
Li-tungstate (1% +Cr)	1.564–1.570	1.561–1.564	0.003–0.006	2.65–2.67
Gilson, yellow-green color	1.564	1.561	0.003	2.65
Gilson, blue-green color (method not disclosed)	1.567	1.562	0.005	2.65
Chatham (method not disclosed)	1.562–1.564	1.559–1.561	0.003	2.65
*Zerfass (method not disclosed)	1.562	1.558	0.003–0.004	2.66
*I.G. Farben, flux, Li-molybdate (Igmerald)	1.562	1.559	0.003	2.65

* Data given by E. J. Gubelin (1964).

Density and optical properties. Densities of hydrothermal and flux emerald were determined by hydrostatic weighing of crystals having weights between 0.5 and 2.0 grams (Table 1). Of more interest to the practicing gemmologist are perhaps the relative densities of synthetic emerald from different sources (Table 2). These values were determined by floating in bromoform small chips of each specimen, gradually diluting with toluene, and observing the individual sinking points. Two test pieces cut from larger crystals whose densities were determined by hydrostatic weighing, served as useful indicators. The refractive indices were determined on either faceted stones or small chips with polished surfaces, using a standard Rayner refractometer and a sodium light source (Table 1). The refractive indices determined for quartz (rock crystal) were found to average 0.002 too low, so this correction figure was added to all subsequent readings.

Before discussing the results it would be advantageous to consider

what factors might affect the density of beryl and emerald. Recent studies on the chemical compositions of natural beryls by Bakakin and Belov (1962) and Schaller *et al*, (1962) have been in agreement that the octahedral positions occupied by Al in the beryl structure may be substituted for by Cr, Fe^{3+}, Fe^{2+}, Mg and Li; alkali and alkaline earth ions occupy the centers of the Si_6O_{18} rings and water molecules lie centrally between the Si_6O_{18} rings in the plane of the Al and Be ions. The extent and exact manner of substitution occurring in the tetrahedral positions occupied by Be and Si is still a matter of controversy. The stuffing of the

TABLE 2. RELATIVE DENSITIES OF SYNTHETIC EMERALD AS DETERMINED BY SUCCESSIVE SINKINGS IN BROMOFORM BY GRADUAL DILUTION WITH TOLUENE

Material	Density
Linde, V_2O_5 beryl, no Cr	
Linde, Li-molybdate emerald	
Quartz, rock crystal	2.651
Gilson emerald, blue-green	
Gilson emerald, yellow-green	
Chatham emerald, flawless prisms	
Linde, V_2O_5 emerald, 1%+ Cr	
Linde, Li-tungstate emerald, 1%+ Cr	
Linde hydrothermal colorless beryl	
Linde hydrothermal emerald, 0.3% Cr	2.678
Linde hydrothermal emerald, 0.6% Cr	
Linde hydrothermal emerald, 0.8% Cr	
Lechleitner beryl-emerald composite (a)	
Linde hydrothermal emerald, 1.2% Cr	
Lechleitner beryl-emerald composite (b)	
Lechleitner fully synthetic emerald (1962)	
Natural aquamarine test piece	2.688
Calcite rhomb	2.710

channels in the beryl structure with alkali ions and water molecules is the major cause of the variation in refractive index and density of natural beryl and emerald. With the synthetic material the situation at present is slightly different. It can be safely assumed that synthetic emeralds are grown in one of two media, anhydrous molten flux or hydrothermal solutions. Emeralds grown from the latter media will henceforth be termed hydrothermal emeralds, and from the former, flux emeralds.

The density and refractive index of synthetic emeralds will, like the natural material, be dependent on the amount of impurity ions and molecules they contain and these are likely to be characteristic of the different

methods of synthesis used. Since the successful experiments of Hautefeuille and Perrey (1888), emerald has been repeatedly grown in anhydrous, alkali-rich, heavy metal-oxide molten fluxes and more recently, probably limited to the last decade, hydrothermally grown emerald has been produced commercially. The possibility of synthetic emerald having its channels stuffed with alkali ions or water molecules is thus quite as probable as it is for pegmatitic beryls. However, analyses of many emeralds grown from anhydrous Li-molybdate (Table 5) and tungstate fluxes, show that the Li_2O values are quite low, <0.05 percent; Mo ranges from 0.08 to 0.18 percent. Impurity concentrations at these levels can probably all be attributed to flux inclusions in the crystal rather than ionic substitution. Not all synthetic emeralds have such a low level of impurities however. For example, an early analysis of Chatham emerald by Rogers and Sperisen (1942) lists the following minor components: Cr_2O_3 2.00, CaO 0.73, MgO 0.10, K_2O 0.21, Na_2O 0.56, H_2O (LOI?) 0.14, TiO_2 0.05 wt.%. The high (for Chatham emerald) refractive indices of $\omega = 1.578$, $\epsilon = 1.573$ and density 2.667 are what might be expected for this chromium level. It would be interesting to know the distribution of the alkali and alkaline earth ions between flux inclusions and channel positions. The unknown acidic component of the flux has not been identified, but traces of Mo detected by emission spectrograph analysis in this Laboratory suggest a molybdate. Gem quality Chatham emerald has much lower chromium ($\leq 1\%$) and impurity levels resulting in somewhat lower and fairly constant refractive indices and density (Table 1).

Appreciable substitution of alkalies in a gem quality (low Cr) flux emerald would certainly raise the refractive index and density into the range of alkali-free hydrothermal (hydrated) emerald or even natural emerald (Table 1). However, such a problem of identification has not yet presented itself as the synthetic emeralds of undisclosed processes of manufacture *viz.*, Chatham, Gilson and Zerfass, all have the lowest refractive indices and density (Table 1). The higher density values recorded for hydrothermal emerald cf. flux emerald are readily explained by the water content of 1 to 2 percent. If one takes as a convenient reference point the density of 2.650 for anhydrous beryl, the effect of water, chromium and alkali substitution on the density may be calculated assuming constancy in lattice dimensions (Table 3). The increase in density due to Cr substitution will probably be less than calculated due to slight expansions of the unit cell. It may be seen that for the limited range of Cr levels required for gem quality emerald (0.2–0.5%) there is at present no overlap between the density values for emerald grown from anhydrous fluxes and that of hydrothermal origin.

A clue that may be helpful in identifying the maker of a faceted syn-

TABLE 3. CALCULATED DENSITIES OF BERYL AND EMERALD

Calculated densities of beryl containing various amounts of Cr substituting for Al and water molecules in the channels, cell dimensions assumed constant.

Material	Density
Beryl, $Be_3Al_2Si_6O_{18}$, anhydrous, no Cr	2.650[1]
Beryl, with 0.2 wt. % Li-molybdate flux inclusion	2.651
Beryl, anhydrous, with 0.5% Cr	2.657
Beryl, anhydrous, with 1.0% Cr	2.664
Beryl, with 1.0% water, no Cr	2.667
Beryl, with 2.0% water, no Cr	2.704
Beryl, with 1.0% water, +0.5% Cr	2.684
Beryl, with 1.0% water +1.0% Cr	2.691
Beryl, with 2.0% water +0.5% Cr	2.711
Beryl, with 2.0% water +1.0% Cr	2.718
Lithium beryl (Na)·Be_2Al·$AlLi$·Si_6O_{18} anhydrous (Li_2O 2.77%, Na_2O 5.79%)	2.753

[1] Assumed density of ideal anhydrous beryl.

thetic emerald is the angle the table facet makes with the *c*-axis of the crystal. Different orientations result from the different habits of emerald crystals grown hydrothermally and from a flux, and due to the probability that the table facet is most often cut parallel with the crystal face having the largest area in order to get the maximum size stone from a given crystal, as well as to avoid having color bands intersecting the crown of the stone.

Flux emeralds are frequently grown on basal seed plates resulting in tabular crystals with hexagonal or dihexagonal prism edges. Faceted stones are usually cut with the table parallel to the basal pinacoid and will show no dichroism when viewed perpendicular to the table, *e.g.*, Gilson and Linde flux emerald. Chatham emerald, on the other hand, is produced as aggregates of hexagonal prisms with flat terminations. Since the crystals tend to be somewhat elongated along the *c*-axis there will be a high probability that stones will be cut with the table paralleling a prism face, as with natural emerald, and will show strong dichroism through the table. Linde hydrothermal emerald is grown on seed plates inclined at an angle to the crystallographic axes. The rough crystals are tabular parallel to two opposing dipyramid faces and are bounded by first- and second-order prism faces; the basal pinacoid is always present but very small and a second-order dipyramid is occasionally developed (Fig. 2). So far, faceted stones have been cut with the table parallel to the first order pyramid which makes an angle of 60° with the *c*-axis. Distinct dichroism is seen through the table.

Inclusions. Examination under high magnification (×400) of the two-phase inclusions present in Linde emerald grown from anhydrous fluxes shows them to be minute cavities filled with solidified flux containing a gas bubble. The Li-molybdate flux is usually in the form of a glass, *i.e.*, it is isotropic, and hence superficially appears to be a liquid. However, the refractive index is readily shown to be much greater than the enclosing

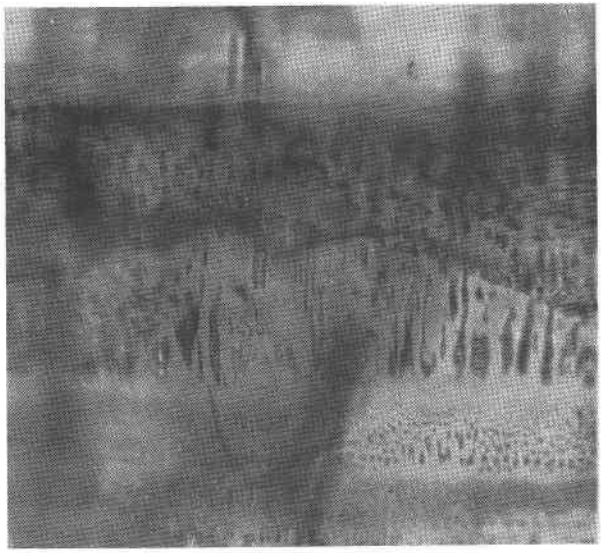

FIG. 3. Photomicrograph of inclusions in Li-molybdate flux grown emerald, section ‖ to the *c*-axis, 150×.

emerald. The boundary of the cavity stands out in high relief as does that of the enclosed gas bubble (Fig. 3). In some of the larger inclusions the glass is partly recrystallized to acicular crystals having a high refractive index and birefringence. The molybdate glass frequently shows irregular tension cracks, particularly if crystallization has started at one end of the inclusion. The glass appears almost colorless; however, any faint color would be obscured by the green of the enclosing emerald. Glass and recrystallized flux of similar appearance were observed in the two-phase inclusions in Chatham, Gilson and Nacken[1] emeralds. The synthetic emerald "Igmerald" of I. G. Farben-Industrie was also grown from Li-molybdate flux (Eppler, 1961), hence glass-filled cavities should be present in these specimens. No samples of Igmerald or Zerfass emeralds were available for examination.

[1] Only one small prism of Nacken emerald of doubtful authenticity was available for examination.

Li-tungstate flux emerald similarly contains colorless glass-filled inclusions, which have exceptionally high relief. Only very minor recrystallization to an acicular phase, having strong birefringence, was observed.

Vanadium pentoxide crystallizes as orange-brown needles having re-

FIG. 4. Photomicrograph of wisp- or veil-like inclusions in V_2O_5 flux-grown emerald. Basal section, 150×.

fractive indices of 1.46, 1.52, 1.76 (orthorhombic). Light absorption by the flux inclusions in V_2O_5 emerald is so strong that crystals much thicker than 1 to 2 mm are almost opaque, hence it is doubtful if any gem quality emerald will be encountered grown from this flux. The inclusions consist predominantly of recrystallized V_2O_5 which is readily identified by its acicular habit, orange-brown color, high refractive index and strong birefringence. The typical wisp or veil-like pattern of inclusions lying along curved surfaces is shown in Figure 4. Some of the very fine, transparent filaments and blebs of flux are isotropic, while adjacent flux in-

clusions of the same size may be birefringent, hence it appears that a small amount of the flux is present as glass. Although V_2O_5 does not form a glass when pure, it is known to do so when containing small amounts of dissolved material (Weyl and Marboe, 1960). The minute size of the individual flux particles ($\sim 10^{-10}$ gm) would also favor glass formation on cooling from the melt.

The two-phase inclusions present in synthetic hydrothermal emerald consist of aqueous fluid and a gas bubble (Fig. 5). They are usually con-

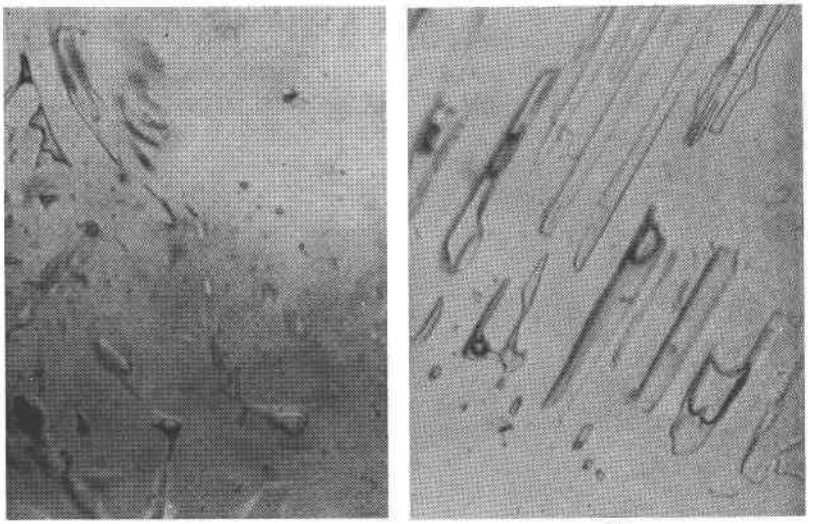

(a) (b)

FIG. 5. Photomicrograph of 2-phase inclusions consisting of liquid and gas, in synthetic hydrothermal emerald, 400×. Irregular shaped voids. Elongated tube-like cavities.

centrated at interfaces associated with interrupted growth periods. Their appearance is similar to the two-phase inclusions seen in natural emerald. The refractive index of the fluid is close to that of water and the degree of relief shown by the cavity wall is noticeably lower than if the filling were a dense molybdate glass (Fig. 3). The Becke line test immediately shows the isotropic filling of the cavity to have a lower refractive index than the host. A lower refractive index recording for an isotropic filling should not be considered as an infallible test for hydrothermal emerald. It may be possible to grow emerald from anhydrous fluxes that on solidifying form a glass or isotropic crystals having a refractive index less than emerald. However, such emeralds have not yet been encountered. In most cases the bubble in the fluid inclusion is rather large and elongated along a tube-like cavity (Fig. 5b). With a heating or cooling stage one could

readily distinguish between a cavity filled with isotropic flux or aqueous fluid when the filling has a lower refractive index than emerald. Tension cracks may sometimes be seen in a glass filling and grain boundaries might be detectable in crystalline isotropic material.

A peculiarity of the two-phase inclusions in synthetic emerald are the cuneiform growth funnels which often start at their widest end on crys-

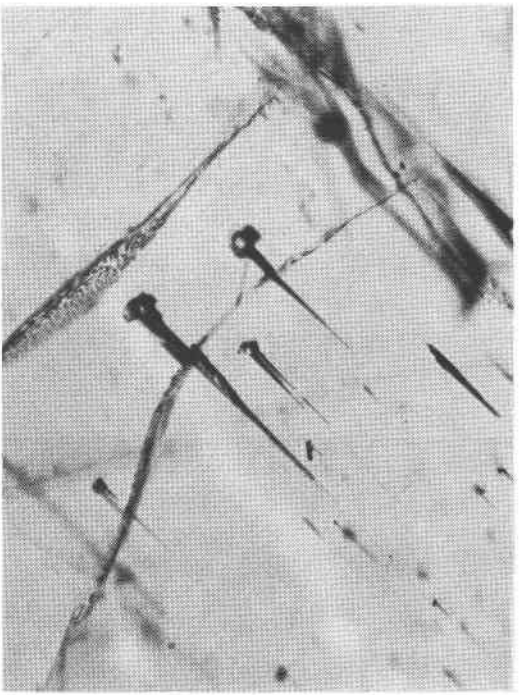

FIG. 6. Photomicrograph of cuneiform growth funnels initiating from crystal inclusions in V_2O_5 flux-grown emerald, 150×.

talline inclusions of some other mineral. The growth funnels taper gradually to a point and tend to parallel the *c*-axis of the crystal (Fig. 6). An examination of both flux and hydrothermal emeralds has shown that these cuneiform openings develop most readily when growth is started on a seed plate inclined at an angle to the crystallographic axes. One reason for using seed plates cut parallel to the basal plane for flux growth of emerald is to avoid this type of defect which in its worst form results in multiple acicular growth along the *c*-axis. Hydrothermal emeralds, however are normally grown on seed plates inclined at an angle to the crystallographic axes hence the cuneiform openings are often present. Acicu-

lar growth develops less readily in the hydrothermal medium than in a molten flux. The observance of cuneiform openings in an emerald is thus not sufficient evidence alone to indicate a hydrothermal origin as suggested by Gubelin (1964).

The most common crystalline inclusion in synthetic emerald is phenacite which is recognized by its habit of usually elongate, colorless hexa-

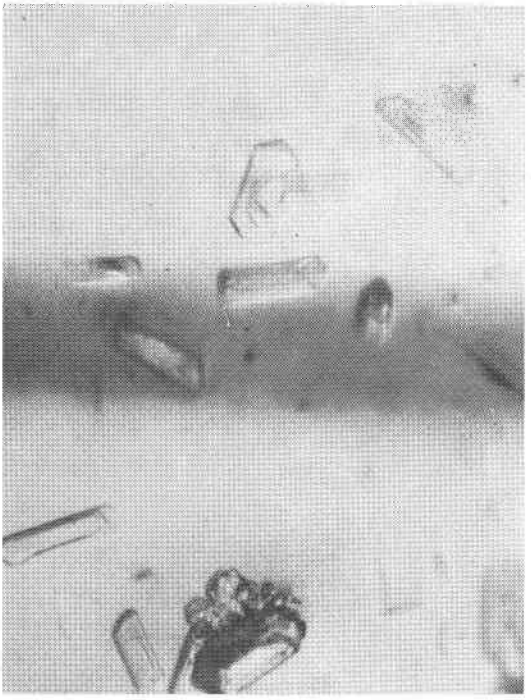

FIG. 7. Photomicrograph of phenacite inclusions in synthetic hydrothermal emerald, 400×.

gonal prisms terminated by rhombohedral faces, and its slightly higher refractive index compared to emerald. It occurs as isolated crystals and also in larger crystalline aggregates frequently localized along a plane. Both Linde flux and hydrothermal emeralds contain occasional phenacite inclusions (Fig. 7).

A different type of crystalline inclusion that may be encountered in synthetic emerald is the seed plate inclusion. Hydrothermal emeralds are grown on seed plates which may be cut from natural beryl or aquamarine. The natural beryl is quite compatible with the hydrothermal medium and suffers no change in physical properties, as might be concluded from examination of a Lechleitner emerald overlay on beryl. In order to get a fully synthetic emerald, once the emerald has grown to a reasonable

thickness on the natural beryl seed plate, two plates of synthetic emerald are sawn free from the natural seed and serve as synthetic seed plates for further growth. A slight color change may sometimes be visible between the synthetic seed plate and new emerald growth when the stone is observed in a liquid of like refractive index.

Flux emerald may be grown initially on seed plates of heat-treated aquamarine as a means of producing synthetic anhydrous emerald seed plates for further production, or by spontaneous nucleation and growth in crystalline aggregates with survival of the fittest being the rule. In the latter case the emeralds show no color banding due to a seed plate, but if they have had an interrupted growth history they may show banding parallel to the hexagonal prism and basal faces of the crystal.

Gilson and Lechleitner emerald. Two Gilson cut stones weighing 0.9 and 1.3 carats were examined, one being a yellowish-green color, the other bluish green. In both, the table facet was parallel to the optic plane. The dichroism was as follows: ω = yellowish-green in both; ϵ = green in yellowish-green stone, ϵ = bluish-green in the other. The larger stone had a dense concentration of phenacite crystals and crystalline aggregates on a plane traversing the stone at the girdle and isolated phenacite prisms randomly distributed elsewhere at low concentration. Veils were abundant above and below the girdle plane and were composed of elongated tube-like flux inclusions. The veils intersected the girdle plane at a steep angle and the flux inclusions, from one veil to the next, tended to be concentrated in bands parallel to the girdle plane. The elongated flux inclusions were in parallel orientation along a veil and pointed towards the *c*-axis which indicates that this was the major growing direction of the crystal. Inclusions of a similar type were present in the smaller stone which also contained three large phenacite prisms measuring 0.35×0.15 mm. The refractive indices of the blue-green stone were higher than the yellow-green stone even though the density of the former was perceptibly lower (Tables 1 and 2). These observations agree well with those of Liddicoat (1964) who shows photographs of typical inclusions in Gilson emerald and rough crystals. The rough crystals photographed are tabular with the basal pinacoids and bounded by hexagonal and dihexagonal prism faces. They are typical in all respects of flux emerald grown on basal plane seed plates. Examples of similar rough and faceted Linde Li-molybdate flux emerald are shown in Figure 1.

A number of recently produced (1964) Lechleitner emerald overlays of natural beryl and also fully synthetic emeralds were examined as well as material of earlier origin (see Holmes and Crowningshield, 1960). The recent emerald overlays are a much deeper green than the earlier ones and

are attractive stones. A very high chromium content is indicated by the high refractive indices and birefringence (Table 1). In one stone the natural beryl contained some hollow tubes about 6μ diameter traversing it, and orientated along the *c*-axis. When the stone was immersed in a liquid of similar refractive index and viewed along the direction of the tubes it appeared colorless since the opposing facets on the crown and pavilion were approximately parallel to the basal plane and had little or no emerald overgrowth. The basal pinacoid and prism faces are the slowest growing for hydrothermal emerald and any facets on the natural beryl preform that closely parallels them will receive a comparatively thin layer of emerald which is usually removed during the subsequent smoothing and polishing of the facets. The usual presence of "windows" in the emerald overlays is thus not deliberately done for easy identification as supposed by Gubelin (1961).

Two recent Lechleitner fully synthetic emeralds weighing 0.46 and 0.44 carats were examined and found to be similar in appearance to the "wafer-type" Lechleitner emerald described by Liddicoat (1964). To be observed internally these emeralds need to be immersed in diluted bromoform or other convenient liquid of similar refractive index. One stone consisted of a colorless seed plate traversing the girdle and had a very thin deep green emerald layer on either side, which rapidly faded into colorless beryl in the direction away from the seed plate and towards the table and base of the stone. The other stone showed a somewhat thick emerald layer but was still characterized by the gradual fading in color in the same directions. The refractometer readings of the colorless beryl on the table gave the lower values expected for synthetic hydrothermal beryl (Table 1). The seed plate contained the same type of inclusions as the outermost colorless layers and therefore there was no reason to suppose that it was not of similar synthetic origin. We prefer to call this type of stone a beryl-emerald composite rather than a wafer or interlayer type, and contrary to the supposition of Liddicoat (1964), believe that only a single seed plate, which is the central colorless band, was used for each stone. Hydrothermal growth of emerald was commenced on the seed plates but after a short time, probably only a few days, the soluble trivalent chromium source was exhausted, thus preventing any further Cr^{3+} substitution in the crystal. The crystal continued to grow however, but as colorless beryl, its predominant composition.

Both stones had the lower pavilion facets cut at angles less than the critical angle in order to get a larger stone than ideally possible from a thin plate. Dichroism is distinct when the stones are viewed through the table facet, and it is apparent that the seed plates used are inclined at an angle to the crystallographic axes. The orientation of the seed plate and

the table facet to the crystallographic axes is likely to be a distinguishing feature between the Lechleitner and Linde hydrothermal emeralds.

Fluorescence properties. Observation of emeralds under ultraviolet light has often been resorted to as a means of differentiating between natural and Chatham synthetic emerald (Webster, 1962). Under long-wavelength ultraviolet (3650 Å), Chatham synthetic emerald shows a red fluorescence much more intense than any natural stone. As an additional aid in identification, the dichromatic Chelsea color filter is sometimes used (Webster, 1962). When viewed through this filter, the Chatham emerald shows a bright red color. Most natural emeralds show a dull deep red color, except those from South Africa and India which remain green; some Colombian emeralds from the Chivor mine show a red color similar to that of the Chatham emerald. Webster (1962) suggests that the reason for the stronger fluorescence in synthetic emeralds is their greater purity and freedom from iron and vanadium which can act as a fluorescence poison to dim or suppress the natural fluorescence due to chromium.

The fluorescence behavior of natural and synthetic emeralds under short- (2537 Å) and long- (3650 Å) wavelength ultraviolet light is indicated in Table 4. Semiquantitative measurements were made of the fluorescence intensity through the Chelsea filter when excited with 2537 Å ultraviolet radiation. In addition, the color observed when viewed through the Chelsea filter under tungsten light is shown. Most emeralds of flux origin show red fluorescent characteristics and a red color through the Chelsea filter. However, the Gilson emerald fluoresces yellow to olive-green and shows a dull red color through the Chelsea filter (Liddicoat, 1964; Gubelin, 1964a; Webster, 1964). Liddicoat (1964) suggests that the unique fluorescent characteristics are related to extraneous ions in the emerald, probably inclusions from the flux. The V_2O_5 flux emerald from this Laboratory shows no red fluorescence, and no red color through the Chelsea filter. The vanadium ions incorporated from the flux apparently quench the fluorescence.

The synthetic hydrothermal emerald from this Laboratory shows a bright red fluorescence under long- and short-wavelength ultraviolet light and a bright red color when viewed through the Chelsea filter under tungsten light. The intensity is greater than any of the other emeralds tested, and serves to distinguish it from the other emeralds. The fluorescence intensity through the Chelsea filter approaches 40 percent that of the strongly fluorescent synthetic ruby (Table 4).

Chemical composition and structure. Chemical analyses were obtained on

a natural Colombian emerald, a Chatham synthetic, a Lechleitner fully synthetic (1962), and two each of hydrothermally grown and flux-grown synthetic emeralds as reported in this paper. Table 5 contains the results of these analyses. The unit-cell contents were calculated by normalizing to 18 oxygen and are included.

TABLE 4. FLUORESCENCE BEHAVIOR OF EMERALDS

Emerald	Fluorescence behavior				
	3650 Å ultraviolet	2537 Å ultraviolet	Fluorescence intensity through Chelsea filter		Color through Chelsea filter[2]
	Visual observation		Arbitrary units[1]		
			Low scale	High scale	
Colombian emerald (0.2% Cr)	None	None	<2	n.d.	No Red
Chatham synthetic emerald:					
(a) Light green, flawless prism	Bright Red		8	39	Bright Red
(b) Dark green, rough	Deep Red		11–14	n.d.	Dull Red
Synthetic hydrothermal emerald (this laboratory):	Bright Red				Bright Red
(a) Rough, 0.7% Cr			19–30	76–120	
(b) Faceted, ~0.7% Cr			25	42–82	
Li-molybdate flux emerald (this laboratory):	Dull Red				Dull red
(a) Rough, ~0.3% Cr			4	n.d.	
(b) Faceted, ~0.1% Cr			6	22	
V_2O_5-flux emerald (this laboratory), 0.4–0.8% Cr	None		0	n.d.	No Red
Lechleitner:					
(a) "Emerita," natural beryl overgrown with synthetic emerald	Pale Red to Red	Pale Red to Bright Red	8	11	Red
(b) Fully synthetic emerald (1962)	None		n.d.	7–10	Red
(c) Beryl-emerald "wafer" composite (1964)	Bright Red				Bright Red
Gilson emerald[3]	Yellow to Olive Green	Yellow to Orange to Olive Green			Dull Red
Zerfass emerald[4]	Red	Red			Bright Red
Synthetic ruby, 0.03% Cr	Brilliant Red		n.d.	270–300	Brilliant Red

[1] Semiquantitative measurements by Mr. L. G. Dowell of this Laboratory. Excited with 2537 Å. ultraviolet radiation, filtered with Chelsea filter, detected with photomultiplier tube.

[2] Illuminated with tungsten light in most cases.

[3] Liddicoat (1964); Gubelin (1964); Webster (1964); and this Laboratory.

[4] Gubelin (1964).

A model of the beryl structure is shown in Figure 8, showing the hexagonal $Si_6O_{18}^{-12}$ rings bonded by means of beryllium in tetrahedral coordination and aluminum in octahedral coordination. The channels along the *c*-axis can be noted. The idealized formula for beryl is $Be_3Al_2Si_6O_{18}$. Bakakin and Belov (1962) presented a comprehensive review of the

TABLE 5. CHEMICAL ANALYSES OF EMERALDS

Wt. %

	Natural Colombian emerald	Chatham emerald	Lechleitner fully synthetic emerald (1962)	Synthetic hydrothermal emerald	Synthetic hydrothermal emerald	V_2O_5 flux emerald	Lithium molybdate-flux emerald
Chemical analyses							
SiO_2	65.6±0.5	66.5±0.5	65.7±0.5	64.9±0.5	67.5±0.5	64.0±0.5	65.7±0.5
Al_2O_3	17.6±0.5	18.4±0.5	18.0±0.5	16.9±0.3	18.8±0.5	19.4±0.3	18.4±0.3
BeO	12.9±0.5	13.8±0.5	13.6±0.5	15.0±0.5	13.4±0.4	15.1±0.5	14.9±0.5
Cr_2O_3	0.3±0.1	1.1±0.1	1.2±0.1	1.56±0.04	0.51±0.04	0.35±0.04	0.26±0.04
Li_2O	<0.06	<0.06					0.05±0.02
Na_2O	1.15±0.05	0.07					
Cs_2O	<0.2	<0.2					
K_2O	<0.04	0.04					
MgO		0.1					
CaO		<0.2					
V						0.15	
MoO_3							0.46±0.03
H_2O	1.9±0.5	—	1.4±0.5	1.0±0.5	1.1±0.2	—	—
Loss on ignition		0.3[1]				0.0	0.3[1]
Unit-cell contents							
Oxides normalized to 18 O's:							
Si	6.07	5.96	6.00	5.91	6.12	5.78	5.91
Al	1.91	1.94	1.93	1.82	1.86	2.06	1.95
Be	2.86	2.97	2.98	3.28	2.93	3.27	3.22
Cr	0.02	0.08	0.09	0.11	0.04	0.03	0.02
V	—		—	—	—	0.02	—
Li	—		—	—	—	—	0.02
Na	0.21	0.01	—	—	—	—	—
Mg	—	0.01	—	—	—	—	—
H_2O:	0.59	—	0.43	0.30	0.33	—	—

[1] Probably a volatile flux component.

crystal chemistry of beryl and proposed rules for the order of filling of the four crystallographic sites as represented below:

	Group I	Group II	Group III	
O_{18} |	(Ring, Tetrahedral)$_6$ |	(Octahedral)$_2$ |	(Tetrahedral)$_3$ ||	Channel

In the ideal structure Group I is filled with Si, Group II with Al and Group III with Be ions. Chromium in emerald substitutes in Group II.

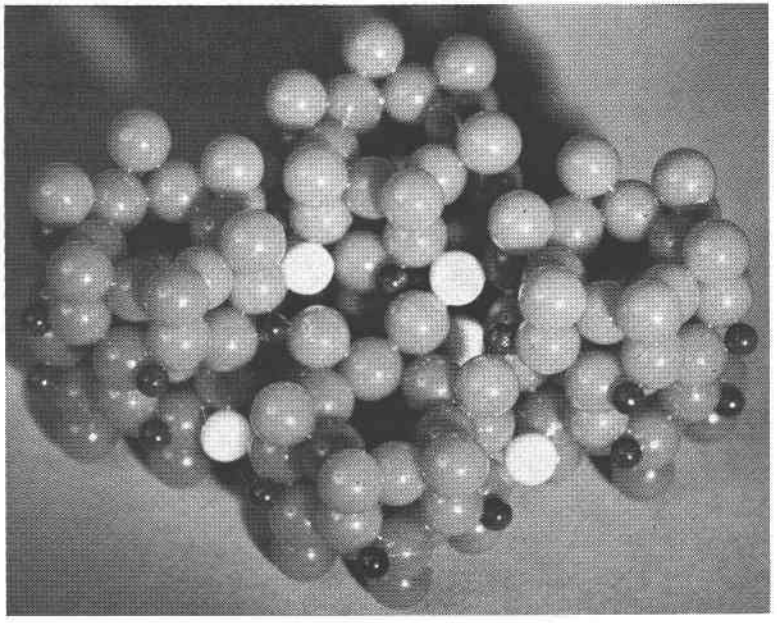

FIG. 8. Model of the crystal structure of beryl. Stacking of hexagonal Si_6O_{18} rings is shown. Oxygen ions are represented by the grey balls. White balls show aluminum ions in octahedral sites. Small dark balls are the Be^{++} ions in tetrahedral sites. Channels formed by the hexagonal rings are evident.

The channel accommodates water molecules and alkali and alkaline earth ions if present. Using the rules proposed by Bakakin and Belov (the reader is referred to their paper for details), the calculated unit cell contents were distributed among the cation sites. These data are shown in Table 6. An excess of beryllium ion over that required to fill Group III is noted in the case of all but one of the hydrothermal and flux emeralds grown in this Laboratory. In one of the synthetic hydrothermal emeralds, the excess required beryllium substitution in all three groups. Similarly, an excess of Be or Si over that required to fill all three groups is observed and assigned to the channel following the filling rules. The order of mag-

nitude of the Si excess is within experimental error of the analyses, but the beryllium seems to be above that value. Since several of the other emeralds analyzed by the same techniques and analysts did not show excess Be or Si, we cannot readily ascribe the discrepancy to analytical error. The coordination of the beryllium ion on the wall of the channel could be favorable. The beryllium ion may be present as an included hydroxylated species. The phenacite and other inclusions present in the synthetic emeralds, particularly in the case of the flux grown where their concentration is significant, could also affect the analyses, resulting in high values of Be or Si.

X-ray diffractometer traces were essentially the same for the natural

TABLE 6. UNIT-CELL COMPOSITIONS OF EMERALDS AFTER BAKAKIN AND BELOV[1]

Colombian Emerald (0.2% Cr)	$O_{18}\vert Si_{6.00}\vert Al_{1.91}Cr_{0.02}\vert Be_{2.86}Si_{0.07}\vert\vert Na_{0.21}\cdot 0.59\ H_2O$ (iron not determined)
Synthetic hydrothermal emerald (1.07% Cr)	$O_{18}\vert Si_{5.91}Be_{0.09}\vert Al_{1.89}Cr_{0.11}Be_{0.07}\vert Be_{3.00}\vert\vert 0.30\ H_2O\ (Be_{0.12})$
Synthetic hydrothermal emerald (0.35% Cr)	$O_{18}\vert Si_{6.00}\vert Al_{1.86}\ Cr_{0.04}\vert Be_{2.93}\ Si_{0.07}\vert\vert 0.33\ H_2O\ (Si_{0.05})$
Li-molybdate flux emerald (0.18% Cr)	$O_{18}\vert Si_{5.91}Be_{0.09}\vert Al_{1.95}Cr_{0.02}Li_{0.02}\vert Be_{3.00}\vert\vert (Be_{0.13})$
V_2O_5 flux emerald (0.24% Cr)	$O_{18}\vert Si_{5.78}Al_{0.11}Be_{0.11}\vert Al_{1.86}Cr_{0.03}V_{0.02}\vert Be_{3.00}\vert\vert (Be_{0.16})$
Chatham emerald (0.8% Cr)	$O_{18}\vert Si_{5.96}Al_{0.04}\vert Al_{1.86}Cr_{0.08}Mg_{0.01}\vert Be_{2.97}\vert\vert Na_{0.01}$
Lechleitner fully synthetic emerald (1962) (0.8% Cr)	$O_{18}\vert Si_{6.00}\vert Al_{1.91}Cr_{0.09}\vert Be_{2.98}Al_{0.02}\vert\vert 0.43\ H_2O$

[1] Bakakin and Belov (1962). Order of occupied sites:
$O_{18}\vert$ (Ring, Tetrahedral)$_6\vert$ (Octahedral)$_2\vert$ (Tetrahedral)$_3\vert\vert$ Channel
All analyses from this Laboratory; normalized to 18 O's.

Colombian emerald, the hydrothermally grown, and the flux grown synthetic emeralds.

Infrared spectra. Infrared spectra were obtained for the hydrothermal and flux emeralds grown in this Laboratory, a Colombian emerald, and a Brazilian aquamarine. The spectra were recorded from 650 to 4000 cm^{-1} on powdered samples (average particle size $<10\mu$) using a KBr wafer technique and Perkin-Elmer Model 21 and Beckman Model IR-4 spectrophotometers with NaCl optics. Care was taken to exclude any water pick-up during the preparation of the KBr wafer. The ground emerald samples were dried at 180°C to remove any surface water as was the KBr powder. The spectra were found to be essentially identical in the 600 to 1500 cm^{-1} region. A typical spectrum of the synthetic hydrothermal emerald is shown in Figure 9. Bands with maxima at 681, 742, 809, 965, 1013 and 1212 cm^{-1} are observed and are in essential agreement with the literature values for beryl, aquamarine and natural emerald (Plyusnina, 1963, 1964; Plyusnina and Bokii, 1958; Saksena, 1961; Pfund, 1945). Variations are observed in the 1500 to 4000 cm^{-1} region in bands associated with hydroxyl groups. Spectra in the 3000

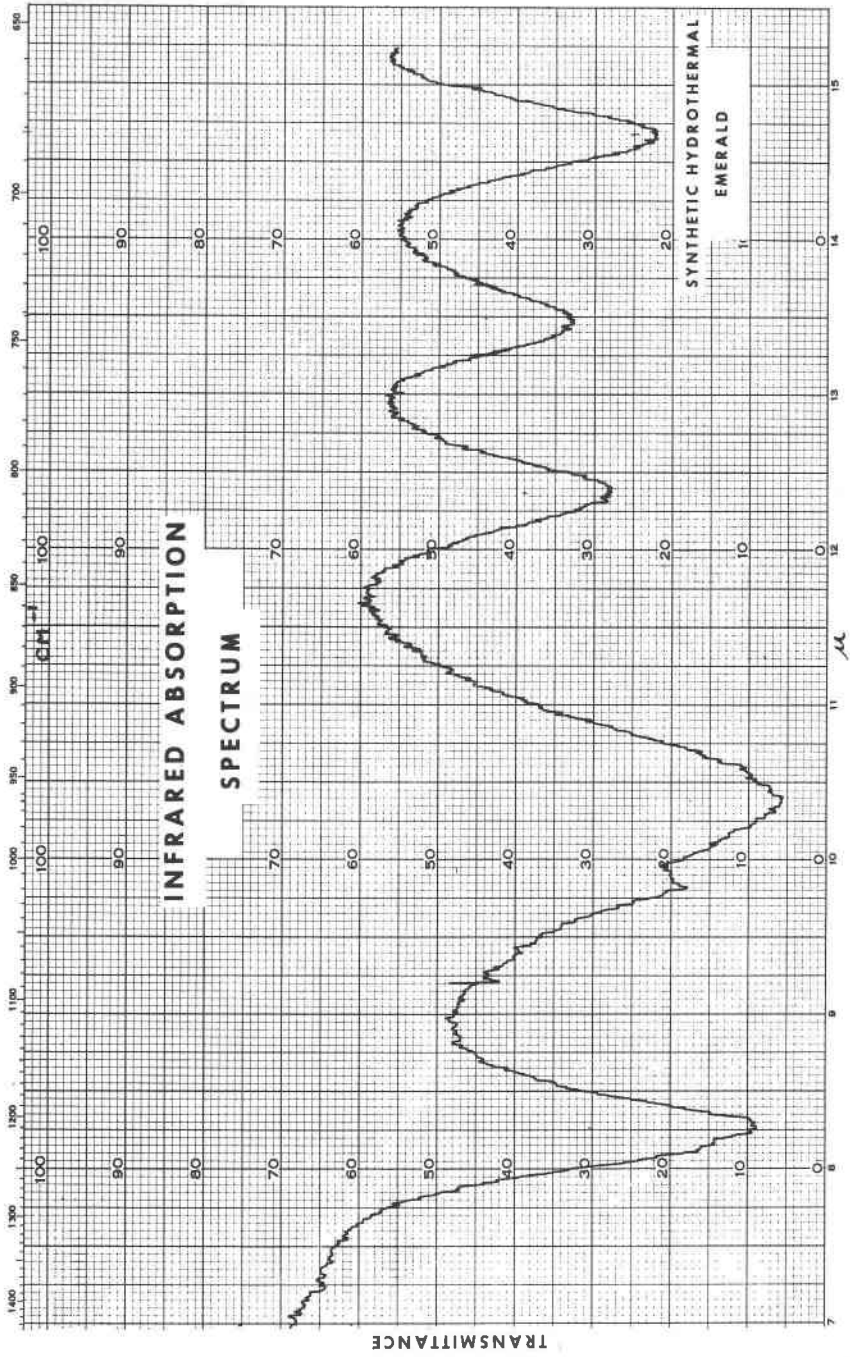

FIG. 9. Infrared spectrum of synthetic hydrothermal emerald from 600 to 1500 cm^{-1}.

to 4000 cm^{-1} region are shown in Figure 10. Those of hydrothermal origin, the synthetic hydrothermal, Colombian emerald and Brazilian aquamarine, show a sharp band at 3690 cm^{-1} and a broad band at 3420 cm^{-1}. In addition to these bands the natural aquamarine and emerald exhibit a sharp band at 3580 cm^{-1} and a broader band at 1630 cm^{-1} (not shown) which are absent in the synthetic hydrothermal emerald. The flux emeralds grown from V_2O_5 and Li-molybdate show only the broad band at 3420 cm^{-1}. The 3420 cm^{-1} band present in all spectra is believed to be extraneous to the sample and related to water pick-up by the KBr during sample preparation despite precautions to prevent it. The intensity of the 3420 cm^{-1} band could not be correlated with emerald concentration in the wafer, and was found to vary randomly with duplicate sample preparations.

In order to verify the spectral differences reported above, additional infrared spectra were obtained later on a Perkin-Elmer Model 621 High Resolution Grating Spectrometer with Fluorolube mulls of the same ground and dried (200°C) samples of two synthetic hydrothermal emeralds, and the natural Colombian emerald. This technique eliminated the presumed extraneous 3420 cm^{-1} band and gave the spectra shown in Figure 11. Sharp OH stretch bands at 3696 cm^{-1} and 3595 cm^{-1} are observed in the Colombian emerald, and a single sharp band at 3699 cm^{-1} in the two synthetic hydrothermal emeralds, essentially duplicating the results from the earlier spectra. An additional weak broad band at 3655 cm^{-1} is observed in the Colombian emerald. In the water deformation region near 1600 cm^{-1}, the Colombian emerald shows sharp bands at 1630 cm^{-1} and 1600 cm^{-1} in the intensity ratio of about 4/1. In the same region the two synthetic hydrothermal emeralds showed only a broad very low intensity hump. All three emeralds showed a significant band at 1545 cm^{-1} with no definite assignment; it may be an overtone or combination frequency.

Determination of the infrared spectra in the 1500 to 4000 cm^{-1} region therefore may be a useful method for identifying the origin of an emerald. The absence of absorption peaks in the 1600–1650 cm^{-1} and 3500–3700 cm^{-1} serve to identify flux emeralds. Emeralds of hydrothermal origin, natural and synthetic, show one or more OH absorption bands. Based on the present data, the synthetic hydrothermal emerald can be distinguished from natural Colombian emerald by the absence of bands near 3600 and 1600 cm^{-1}. A more extensive selection of specimens of known origin needs to be examined to verify the distinction between natural and synthetic hydrothermal emeralds, and to judge the usefulness of this technique.

The assignment of OH frequencies observed in emeralds and other

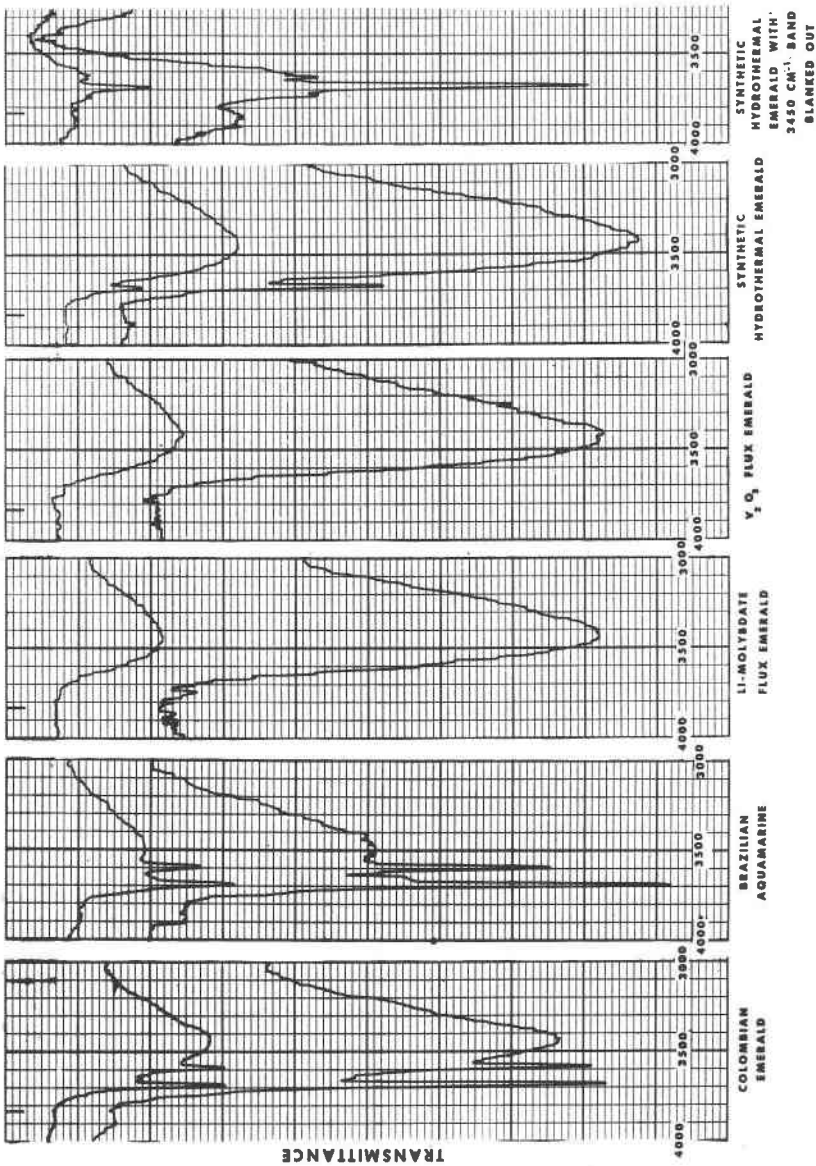

FIG. 10. Infrared spectra of emeralds in OH region, 3000 to 4000 cm^{-1}.

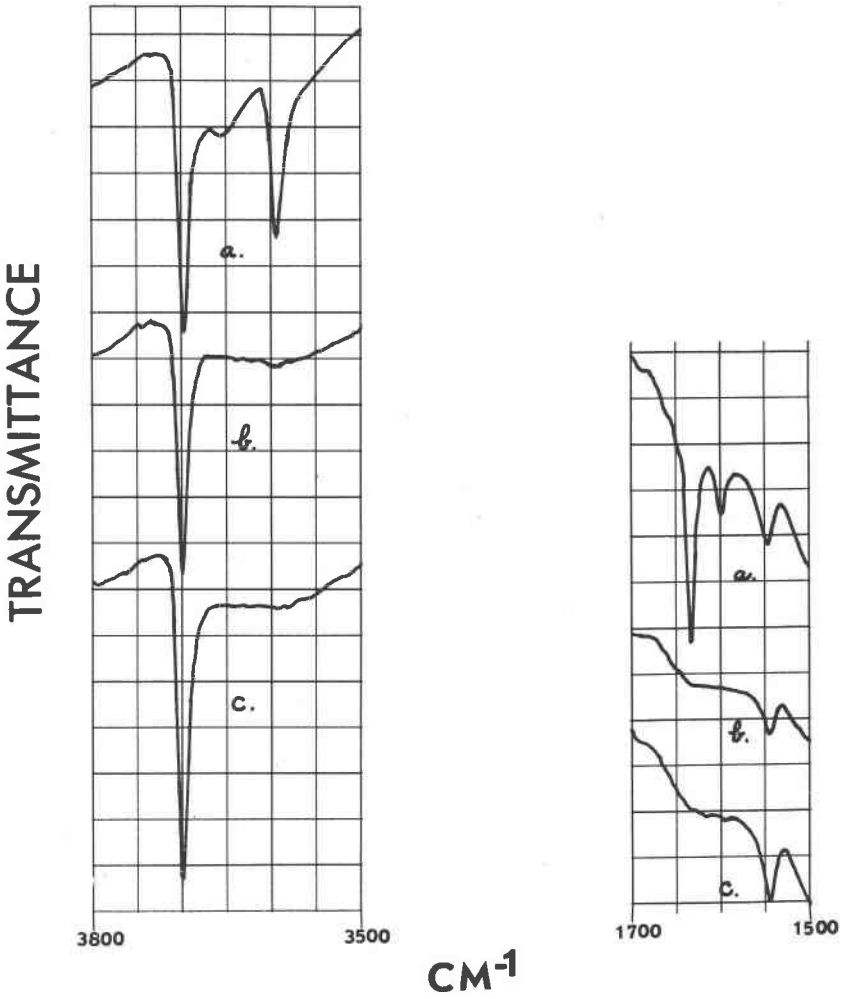

FIG. 11. High resolution spectra of emeralds in OH regions, 3400 to 3800 cm^{-1} and 1500 to 1700 cm^{-1}: a. Colombian emerald; b. and c. synthetic hydrothermal emerald.

beryl analogues requires some further clarification. Bands near 3600, 3700 and 1600 cm^{-1} in natural beryl and aquamarine have been observed by most investigators (Matossi and Bronder, 1938; Lyon and Kinsey, 1942; Wickersheim and Buchanan, 1959; Saksena, 1961). Lyon and Kinsey (1942) attribute both the 3598 and 3690 cm^{-1} bands to OH stretch frequencies of monomeric water in the beryl channel. Boutin *et al* (1964, 1965) studied the OH in beryl by means of neutron inelastic scattering and Paré and Ducros (1964) by nuclear magnetic resonance

techniques. Their results are also consistent with monomeric water molecules in the channel. Paré and Ducros find no evidence of structural OH. On the other hand, Matossi and Bronder (1938), and Wickersheim and Buchanan (1959, 1965) suggest the presence of hydroxyl groups in addition to water. The hydroxyl groups can be alkali or alkaline earth hydroxides lying lengthwise in the beryl channel as first suggested by the latter authors, or hydroxyl ions substituted for oxygens in the silicate ring as suggested by Warner *et al* (1959) and recently by Wickersheim and Buchanan (1965). Proton magnetic resonance studies by Sugitani *et al* (1966) indicate the existence of two kinds of protons in a natural beryl, one a molecular form of water in the channel, and the other a hydroxyl ion replacing O^{2-} ion in the lattice with the proton-proton line of the water parallel to the *c*-axis of the crystal. The present data do not resolve the difficulty in interpretation of OH frequencies. The presence of the sharp 3699 cm^{-1} band and absence of any significant 1600 to 1630 cm^{-1} deformation band of water in the synthetic hydrothermal emerald suggests an assignment to a cation-hydroxyl group. The cation must be one of the framework ions, since there are no alkali or other alkaline earth ions in the synthetic emerald. The 3696 cm^{-1} band could alternatively arise from alkali or alkaline earth hydroxide in the natural aquamarine and emerald. The assignment of the 3595 cm^{-1}, and 1600 and 1630 cm^{-1}, to the stretching and deformation frequencies respectively for water seems most reasonable. Akhmanova, *et al* (1963) report an absorption band at 1400–1470 cm^{-1} due to hydroxyl groups at the vertices of XO_4 tetrahedra in a large number of silicate structures, *e.g.* garnet. There was no evidence of bands in the 1400–1470 cm^{-1} region in emeralds or aquamarine in the present work, although the framework cation-hydroxyl assignment of the 3699 cm^{-1} band in the synthetic hydrothermal emerald might be expected to show the 1400 cm^{-1} band of Akhmanova.

Discussion and Conclusions

The properties of emeralds define the nature of their origin, natural, synthetic fluxmelt or synthetic hydrothermal. Those characteristic of each type of emerald are summarized in Table 7. Synthetic emeralds crystallized from molten fluxes can be identified most readily by their low refractive indices (1.56–1.57), birefringence (0.003–0.005), and density (2.65–2.67). Other definitive characteristics are: wisp-or veil-like two-phase inclusions containing solidified flux and a gas bubble, the refractive index of the glass or crystallized flux inclusion being appreciably higher than that of emerald; an infrared spectrum free of any hydroxyl group absorption in the 4000 to 1600 cm^{-1} region. Synthetic

hydrothermal emeralds have higher refractive indices (1.57–1.58), birefringence (0.005–0.006), and density (2.67–2.69); exhibit bright red fluorescence under ultraviolet light; show a bright red residual color through the Chelsea filter; contain two-phase inclusions, often elongated, of liquid and gas, the refractive index of the liquid being close to that of water; exhibit at least one infrared absorption band in the OH stretch frequency region of 3600 to 3700 cm^{-1}. Although many of the properties of natural emeralds are close to those of the synthetic hydrothermal emeralds (*e.g.* refractive index, birefringence and density), some of the

TABLE 7. CHARACTERISTIC PROPERTIES OF EMERALDS[1]

	Natural emeralds	Synthetic emeralds	
		Flux-melt	Hydrothermal
Refractive index range	1.57 –1.59	1.56 –1.57	1.57 –1.58
Birefringence	0.005–0.007	0.003–0.005	0.005–0.006
Specific gravity	2.68 –2.77	2.65 –2.67	2.67 –2.69
Fluorescence (UV) Short, 2537 Å Long, 3650 Å	None to distinct red	Variable, depends on flux. None, yellow to green, or dull red to bright red.	Bright red
Residual color through Chelsea filter	None, to bright red (rare).	Usually bright red; varies with flux to no red.	Bright red
Inclusions and microstructures	2- and 3-phase inclusions, gas, liquid, salt crystal. Inclusions of actinolite, mica, or pyrite crystals.	Wisp- or veil-like 2-phase inclusions, solidified flux and gas; phenacite inclusions; possibly seed plate discontinuity.	2-phase inclusions, liquid and gas; occasional phenacite inclusions; possibly seed plate discontinuity.
Infrared Spectrum	OH bands (Three OH bands in region of 3700 cm^{-1}, 3600 cm^{-1} and 1600 cm^{-1})[2]	No OH bands	OH band (Single OH band near 3700 cm^{-1}).[2]

[1] Data from this Laboratory and Holmes and Crowningshield (1960).

[2] Tentative conclusion, requires verification with other specimens of known origin of natural and synthetic hydrothermal emeralds. However, any emerald of hydrothermal origin would be expected to contain OH groups (water and/or hydroxyl) giving rise to OH bands in the infrared region of 4000 cm^{-1} to 1500 cm^{-1}.

following distinctions may serve to identify them: dull to no red fluorescence under ultraviolet light and dull red color through the Chelsea filter with certain exceptions; more than one infrared absorption band due to hydroxyl groups in the 1500 cm^{-1} to 4000 cm^{-1} region (needs verification). The most valuable property for positively identifying natural emeralds still remains the nature of the inclusions, *e.g.*, the presence of crystal inclusions such as actinolite, mica and pyrite, and of three-phase inclusions (gas, liquid, salt crystal). The minor element content and distribution may also serve to distinguish an emerald of natural origin from one of synthetic origin. No study of this point was made in

this work,[1] but in general synthetic emeralds should have a smaller number of minor elements and a distribution different from that of natural emeralds.

Based on the characteristics described here and in the literature and the criteria developed above, all of the known synthetic emeralds produced in reasonable size and frequency over the last several decades, can be classified as flux-melt grown: Igmerald, Chatham, Gilson and Zerfass. The new hydrothermal emerald reported here from this Laboratory appears to be the only available synthetic emerald grown hydrothermally. Based on literature reports, the Nacken emerald would also be classified as hydrothermal. The Emerita synthetic emerald overlay on natural beryl and the beryl-emerald wafer composite of Lechleitner are of hydrothermal origin but cannot be properly classified as emeralds.

The development of a hydrothermal process to produce large emeralds has resulted in crystals with optical quality and color superior to any fluxmelt grown emeralds and comparable to the finest first grade gemstones from Colombia or the Ural Mountains. The excellent quality is inherent of hydrothermally grown crystals. Previously, hydrothermal crystal growth techniques had only been applied to simple oxide systems such as SiO_2 (quartz), Al_2O_3 (ruby, sapphire), and ZnO to produce crystals of any reasonable size and quantity. A successful hydrothermal process for growth of large emerald crystals encourages the extension of of hydrothermal techniques into the realm of complex oxides which are difficult to grow by fusion methods and which may be of potential interest for use as gemstones and solid state materials.

Acknowledgements

The authors are grateful to Mr. Lester G. Dowell who carried out the X-ray and fluorescence measurements, Miss Barbara A. Bierl for the infrared measurements, and Mr. Robert G. Pankhurst for the chemical analyses. We also acknowledge the helpful suggestion of Dr. E. Wm. Heinrich with regard to the minor element distribution in natural emeralds.

References

Akhmanova, M. V., A. V. Karyakin, and G. V. Yukhnevich (1963) Determination of hydroxyl groups in silicate minerals by infrared spectrophotometry. *Geochemistry* **1963,** 596–600.

Amstutz, A. and A. Borloz (1935) Synthesis of emerald. *Arch. Sci. Phys. Nat.* **17,** *Suppl.* 39–41 [*Chem. Abs. 1936,* **30,** 2513.]

Anderson, B. W. (1935) Igmerald—the German synthetic emerald. *Gemmologist* **4,** 295.

[1] Dr. E. Wm. Heinrich suggested consideration of the minor element differences in natural emeralds.

BAKAKIN, V. V. AND N. V. BELOV (1962) Crystal chemistry of beryl. *Geochemistry* **1962,** 484–500.

BOUTIN, H., G. J. SAFFORD, AND H. R. DANNER (1964) Low-frequency motions of H_2O molecules in crystals. *J. Chem. Phys.* **40,** 2670–2679.

———, H. PRASK AND G. J. SAFFORD (1965) Low-frequency motions of H_2O molecules in beryl from neutron inelastic scattering data. *J. Chem. Phys.* **42,** 1469–1470.

EBELMAN, M. (1848) Sur une nouvelle methode pour obtenir des combinations cristallisees par la voie seche, et sur ses applications a la reproduction des especes minerales. *Ann. Chimie Phys.*, **22,** 213–244.

EPPLER, W. F. (1961) Synthetic emerald *J. Gemmol.* **8,** 88–95.

EMEL'YANOVA, E. N., S. V. GRUM-GREZHIMAILO, O. N. BOKSHA, and T. M. VARINA (1965) Artificial Beryl Containing V, Mn, Co, and Ni. *Sov. Phys. Crystallog.* **10,** 46–49.

ESPIG, H. (1960) Die Synthese des Smaragds. *Chem. Tech.* **12,** No. 6, 327–31.

——— AND M. JAEGER (1935) Synthetic emerald. *Deut. Goldschmiede-Ztg.* **38,** 347–9.

FEKLICHEV, V. G. (1963) Chemical composition of minerals of the beryl group, character of isomorphism, and position of principle isomorphous elements in the crystal structure. *Geochemistry* **1963,** 410–421.

GENTILE, A. L., D. M. CRIPE, AND F. H. ANDREW (1963) The flame fusion synthesis of emerald. *Amer. Mineral.* **48,** 940–943.

GOODWIN, F. E. (1961) Maser action in emeralds. *J. Appl. Phys.* **32,** 1624–25.

GUBELIN, E. J. (1964) Zwei neue synthetische Smaragde. *Z. Deut. Ges. Edelsteinkunde* **47,** 1–10.

——— (1964a) Two new synthetic emeralds. Gems Gemol. **11** 139–148.

——— (1961) Hydrothermal rubies and emerald-coated beryl. *J. Gemmol.* **8,** 49–63.

HAUTEFEUILLE, P. AND A. PERREY (1890) Sur les combinaisons silicatees de la glucine. *Ann. Chim. Phys.* **20,** 447–480.

——— AND A. PERREY (1888) Sur la reproduction de la phenacite et de l'emeraude. Academie des Sciences. *Acad. Sci. Paris* **106,** 1800–03.

HOLMES, R. J. AND C. R. CROWNINGSHIELD (1960) A new emerald substitute. *Gems Gemol.*, spring 1960, 11–22.

LEFEVER, R. A., A. B. CHASE, AND L. E. SOBON (1962) Synthetic emerald. *Amer. Mineral.* **47,** 1450–53.

LIDDICOAT, R. T. (1964) Developments in the synthetic emerald field. *Gems Gemol.* 131–148.

LINARES, R. C., A. A. BALLMAN, AND L. G. VAN UITERT (1962) Growth of beryl single crystals for microwave applications. *J. Appl. Phys.* **33,** 3209–10.

LYON, W. AND E. L. KINSEY (1942) Infra-red absorption spectra of the water molecules in crystals. *Phys. Rev.* **61,** 482.

MATOSSI, F. AND O. BRONDER (1938) The infrared absorption spectrum of several silicates. *Z. Phys.* **111,** 1.

MILLER, R. P. AND R. A. MERCER (1965) The high-temperature behaviour of beryl melts and glasses. *Mineral. Mag.* **35,** 250–276.

PARÉ, X. AND P. DUCROS (1964) A study of water in beryl by nuclear magnetic resonance. *Bull. Soc. Franc. Mineral. Cristollogr.* **87,** 429–433.

PFUND, A. H. (1945) The identification of gems. *J. Opt. Soc. Amer.* **35,** 611.

PLYUSNINA, I. I. (1964) Infrared absorption spectra of beryls. *Geochemistry* **1964,** 13–21.

——— (1963) Infrared absorption spectra of beryllium minerals. *Geochemistry* **1963,** 174–190.

——— AND G. B. BOKII (1958) The infrared reflection spectra of the cyclosilicates in the wavelength interval from 7–15μ. *Sov. Phys. Crystallogr.* 761–764.

ROGERS, A. F. AND F. J. SPERISEN (1942) American synthetic emerald. *Amer. Mineral.* **27,** 762–68.

SAKSENA, B. D. (1961) Infra-red absorption studies of some silicate structures. *Trans. Far. Soc.* **57,** 242–55.

SCHALLER, W. T., R. E. STEVENS, AND R. H. JAHNS (1962) An unusual beryl from Arizona. *Amer. Mineral* **47,** 672–699.

SCHIEBOLD, E. (1935) Comparative investigation of natural and synthetic emerald. *Z. Kristallogr.*, **92,** 435–73.

SCHLOSSMACHER, K. (1963) Eine neue Smaragdsynthese. *Z. Deut. Ges. Edelsteinkunde* **43,** 27–29.

SUGITANI, Y., K. NAGASHIMA AND S. FUJIWARA (1966) The NMR analysis of the water of crystallization in beryl. *Bull. Chem. Soc. Jap.* **39,** 672–674.

TRAUBE, H. (1894) Briefliche Mittheilungen an die Redaction. *Jahrb. Mineral.* **1,** 275–277.

VAN PRAAGH, G. (1947) Synthetic quartz crystals. *Geol. Mag.* **84,** 98–100.

WARNER, L., W. HOLSER, V. WILMARTH, AND E. CAMERON (1959) Non-pegmatite beryllium sources of the United States. *U. S. Geol. Surv. Prof. Paper* **318.**

WEBSTER, R. W. (1964) The French synthetic emerald, *J. Gemmol.* **9,** 191–196.

——— (1962) *Gems.* Vol. **1,** Butterworths and Company, Ltd., London, p. 322.

WEYL, W. A. AND E. C. MARBOE (1960) Conditions of glass formation among simple compounds. *Glass Ind.* **41,** 429–33, 463–4, 487–91, 526–7, 549–53, 590, 620–7, 658–9.

WICKERSHEIM, K. A. AND R. A. BUCHANAN (1959) The near infrared spectrum of beryl. *Amer. Mineral.* **44,** 440–445.

——— (1965) Some remarks concerning the spectra of water and hydroxyl groups in beryl. *J. Chem. Phys.* **42,** 1468–1469.

WILSON, W. (1965) Synthesis of beryl under high pressure and temperature. *J. Appl. Phys.* **36,** 268–270.

Manuscript received June 28, 1965; accepted for publication February 25, 1967.